

Review

DNA Aptamers for Functionalisation of DNA Origami Nanostructures

Yusuke Sakai¹, Md. Sirajul Islam¹, Martyna Adamiak¹, Simon Chi-Chin Shiu², Julian Alexander Tanner² and Jonathan Gardiner Heddle^{1,*}

¹ Malopolska Centre of Biotechnology, Jagiellonian University; yusuke.sakai@uj.edu.pl (Y.S.); md.sirajul.islam@uj.edu.pl (M.S.I.); martyna.adamiak@uj.edu.pl (M.A.); jonathan.heddle@uj.edu.pl (J.G.H.)
² School of Biomedical Sciences, Li Ka Shing Faculty of Medicine, The University of Hong Kong; simon.chichin.shiu@gmail.com (S.C.C.S.); jatanner@hku.hk (J.A.T.)
* Correspondence: jonathan.heddle@uj.edu.pl; Tel.: +48-12-664-6119

Abstract: DNA origami has emerged in recent years as a powerful technique for designing and building 2D and 3D nanostructures. While the breadth of structures that have been produced is impressive, one of the remaining challenges, especially for DNA origami structures intended to carry out useful biomedical tasks in vivo, is to endow them with the ability to detect and respond to molecules of interest. Target molecules may be disease indicators or cell surface receptors, and the responses may include conformational changes leading to release of therapeutically relevant cargo. Nucleic acid aptamers are ideally suited to this task and are beginning to be used in DNA origami designs. In this review we consider examples of uses of DNA aptamers in DNA origami structures and summarise what is currently understood regarding aptamer-origami integration. We review three major roles for aptamers in such applications: protein immobilisation, triggering of structural transformation, and cell targeting. Finally, we consider future perspectives for DNA aptamer integration with DNA origami.

Keywords: DNA origami; aptamer; DNA nanotechnology; protein nano array; biosensor; logic gate; enzyme cascade; drug delivery system; targeted therapy; molecular robotics

1. Introduction

Nucleic acid aptamers are typically 15-90 nucleotide lengths of single-stranded DNA, RNA or modified nucleic acid, which can function similarly to antibodies – having the ability to bind to molecular targets with high specificity and affinity. They are selected from a random sequence pool according to affinity for a particular target by several rounds of selection and amplification in a process known as Systematic Evolution of Ligands by EXponential enrichment (SELEX) (Figure 1) [1, 2]. This was originally carried out using RNA but single-stranded DNA (ssDNA) was shown to be viable in work that developed a thrombin aptamer [3]. The use of DNA has a number of advantages over RNA, notably higher chemical stability and obviation of a reverse transcription step during each round of SELEX, concomitantly DNA aptamer development has grown rapidly [4]. Perhaps surprisingly, although RNA has the additional 2'-hydroxyl group which imparts more diverse secondary structures than DNA, successful aptamers of both types have been shown to have affinities comparable to monoclonal antibodies (K_D in the range 0.1-50 nM [4]). Taking advantage of the fact that aptamers are synthesised chemically, varieties of chemical modifications have been introduced to the base, ribose and phosphate backbone to confer chemical stabilities, options for further chemical conjugation and higher affinities[5]. For example, 2'-fluoro,2'-amino and 2'-O-alkyl substitution of ribose are well-known to increase nuclease stability[6, 7] while introducing amino acid mimicking bases has been demonstrated to expand chemical diversity of aptamer structures [8, 9].

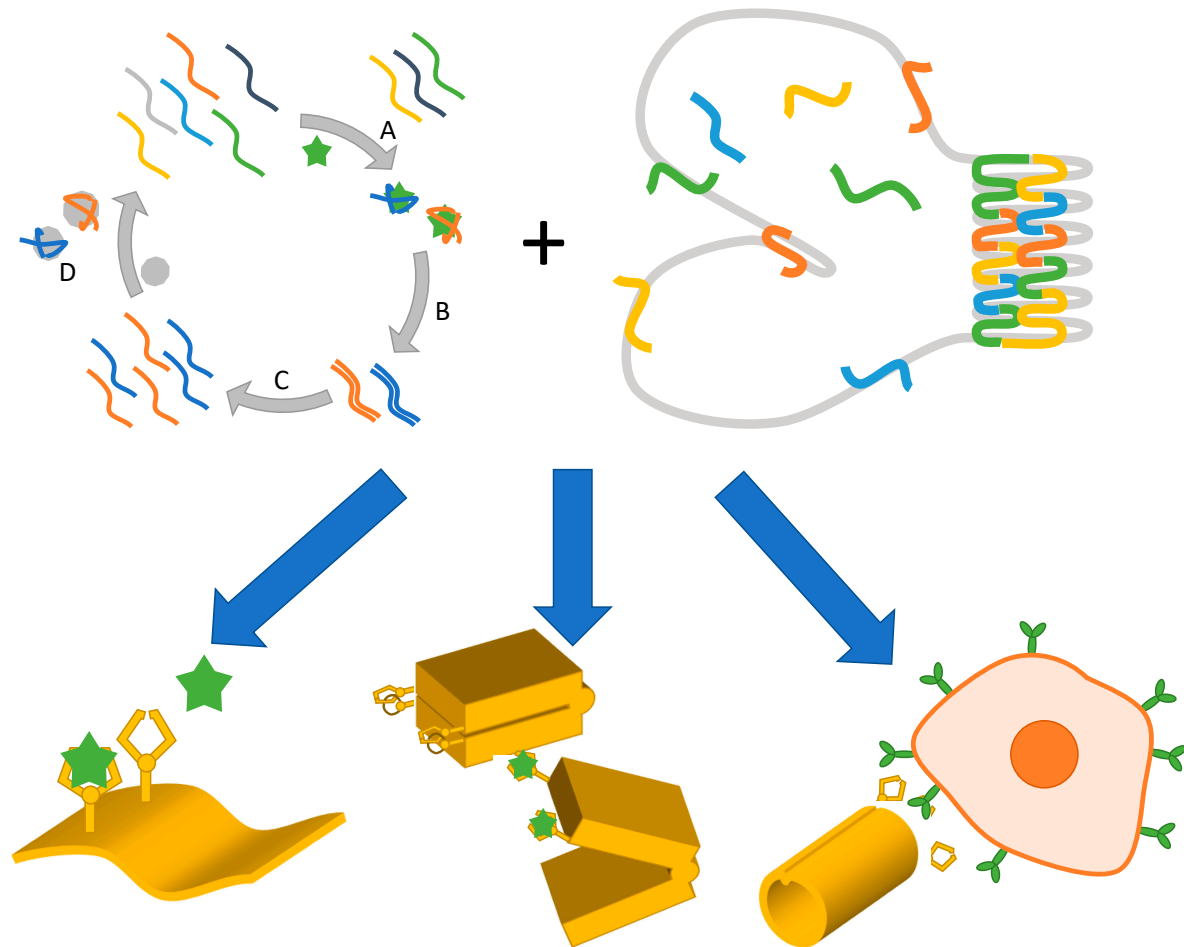


Figure 1. Applications of DNA aptamers when combined with DNA origami. (Top left) Schematic of the SELEX process. First, the fraction with target (green star) affinity is extracted from an initial ssDNA/RNA pool (A) and amplified by (reverse transcription and) PCR amplification (B). The reverse sequences are removed, or forward sequences are transcribed to prepare an enriched ssDNA or RNA library respectively (C) and occasionally counter selection is inserted to remove non-specific binding fractions according to affinity for counter target (grey circle) (D). The selected fraction is used as the second-generation library for the next round of selection (A). **(Top right)** Schematic illustration of DNA origami assembly. A long ssDNA (grey) is folded by hundreds of short ssDNA (coloured) by designed hybridization. Combination of aptamer and DNA origami can result in: **(Bottom left)** protein nanoarray and biosensor construction via capture of target protein by aptamer arm; **(Bottom centre)** Target dependent mechanical transformation by aptamer-lock or split aptamer integration for either biosensing or molecular computing; and **(Bottom right)** specific cell targeting for drug delivery and targeted therapy e.g. by utilising cancer cell targeting aptamers.

As for antibodies, aptamers have potential for targeted therapy, triggering cell signalling, or inhibition of the enzymatic activity of target molecules. Aptamers can be readily chemically synthesized and modified, leading to the expectation of reduced quality control costs for medical usage when compared to antibodies. Further advantageous characteristics of nucleic acid aptamers include flexibility of chemical modification, long storage period and low immunogenicity. Conjugation to other chemical entities has been demonstrated including chemotherapeutic agents, siRNA, nanoparticles, and solid phase surfaces for therapeutic and diagnostic applications[5]. A notable example of practical use is Macugen, an RNA aptamer that was the first Food and Drug Administration (FDA) approved drug used in the treatment of macular degeneracy disease[10, 11]. Several aptamer therapeutics for oncology have shown promise in pre-clinical models as well as

clinical trials[12]. Aptamers are also being developed that can be used as clot busters, cancer therapies, autoantibodies, diabetes treatments, etc[13].

DNA origami (also herein referred to as simply “origami”) is a method whereby arbitrary 2D and 3D nanoscale objects made from DNA can be designed and produced in a relatively straightforward way (Figure 1) and was first introduced in 2006[14]. DNA origami structures are made from a template strand of ssDNA, typically M13 phage genomic DNA which is folded into shape by many (typically around 200) short staple strands which are complementary to linearly distal sequences of the template strand. Maximisation of base-pairing to the staple brings the distal sequences into close proximity and in this way a bespoke shape can be formed. DNA origami has progressed rapidly and a breath-taking array of structures have been produced[15]. 2D DNA origamis have been widely used, for example to produce nanoscale imagery[14, 16] as well as structures with potential applications such as molecular pegboards[17-20], molecular rulers [21, 22] and to produce heterogeneous arrays of proteins in nanoscale wells[23]. 3D DNA origamis[24] have been produced with a wide range of sizes, shapes and decorations. These have been shown to be able to act as nanocontainers[25], immunomodulating agents[26], computational devices, standards in electron microscopy[27], amongst many others.

As DNA origami and DNA/RNA aptamers are constructed from nucleic acid material they offer an immediate compatibility with DNA origami whereby aptamers could be attached to any extended staple sequence via base pairing or via simple extension of the staple sequence. Aptamers can potentially be placed anywhere on a DNA origami structure with high resolution due to the fact that the DNA helices in DNA origami structures are bundled tightly together with the centres of neighbouring helices being only ca 2 nm apart and the phase of the double helical phosphate backbone of the staple stands to which the aptamers attach repeats with a ca 3 nm pitch. It is also the case that each staple strand could in theory be appended with a different bound molecule allowing for multiplexing of functionalities.

DNA aptamers have found a myriad of uses outside of their use in DNA nanotechnology [28]. For example, they have been attached to gold nanoparticles whereby the presence/absence of ligands such as lead, adenosine, cocaine or mixtures can control the accessibility of complementary sequences on the nanoparticles leading to “switching on” or “off,” resulting in observable colour changes [29, 30]. Aptamers responsive to ATP have been used to decorate polymers to deliver doxorubicin, an anti-cancer drug, designed to be released in the cell due to ATP aptamer transformation [31, 32].

The realm of DNA origami research is a part of a vast field of DNA nanotechnology and there are numerous reports of aptamer functionalised DNA nanostructures [33-38]. Though still at a relatively early stage, three principles of successful aptamer integration design for DNA nanostructures have recently been outlined: Shape – overall design of DNA nanostructure to define how and for what purpose aptamer modules are integrated; Self-Complementarity – an indispensable optimisation step to control equilibration between the two states of the aptamer in presence or absence of target molecule; Spatial Flexibility – optimal positioning of aptamers to give accessibility and or space for the DNA nanostructure itself to undergo dynamic movement [39]. As more aptamers are developed, they will represent a growing library of motifs that may be incorporated into DNA origami structures. Here, we highlight specific examples of DNA origami research as well as milestone reports of individual methodologies to give a snapshot of current research and future perspectives of the marriage between DNA origami and nucleic acid aptamers.

Overall, DNA and RNA aptamers offer significant opportunity for facile attachment to designed DNA origami structures in order to endow them with useful functionality. Existing research points at the possible categories of aptamer modifications that may be used and these include i) aptamers to immobilise target molecules, as demonstrated by nanoarrays as well as biosensor applications (Figure 2); ii) using aptamers to trigger DNA nanostructure conformational changes aimed at either biosensor or molecular computing outcomes (Figure 3); iv) using aptamers for (cancer) cell targeting for drug delivery (Figure 4).

2. Aptamers for Target Immobilization

DNA nanotechnology has offered an exquisite method for producing bottom-up nanoarrays, i.e. it can be used to organize various particles in spatially defined patterns with nano-meter precision via self-assembly, as first demonstrated by the construction of simple nanostructures of gold nanoparticles precisely arrayed on a DNA helix[40]. Using biotinylated DNA has allowed templated nanoarrays to expand to include streptavidin[41] and streptavidin coupled antibodies [42]. A more universal methodology of DNA based protein nanoarray formation was subsequently shown[43] where a 15 nt thrombin aptamer (HD1)[3] was successfully introduced which precisely arrayed thrombin on triple-crossover DNA tiles as observed by atomic force microscopy (AFM). These arrayed nanoparticles are typically visualised by AFM as dot(s) of appropriate height on regularly patterned DNA nanostructures as if target molecules are pegged by aptamer on pegboard made of DNA.

In 2007, just after the introduction of the DNA origami method, the platform of aptamer based protein nano-arrays was expanded from DNA tiles [43] to DNA origami (Figure 2A)[17]. A platelet derived growth factor (PDGF) aptamer (36t) [44] and a thrombin aptamer (HD22)[45] were each arrayed on a rectangular DNA origami structure with nanometre precision. This multivalent aptamer system was further systematically investigated [46]: one target molecule was captured on the DNA nanostructure by two aptamers recognising different epitopes using another thrombin aptamer (HD1)[3]. Utilising the precise addressability of the DNA nanostructure, 4-helix bundle or 5-helix bundle DNA tiles and the rectangular DNA origami, two thrombin aptamers were arrayed with a separation varying from 2 to 6.9 nm in order to seek the optimal interval for the efficient binding of thrombin, verified by EMSA. A four-thymine spacer was added to the ends of the aptamers to increase flexibility. As the two aptamers recognise the opposite sides of the ca 4.1 diameter protein simultaneously, the optimal spacing of the aptamers was found to be 5.3 nm, i.e. four dsDNA helices. Combining a microfluidics system and the DNA origami with dual thrombin aptamers resulted in a biosensor system for rapid detection of thrombin from cell lysate (Figure 2B)[47]. In this work, a simple crossed microchip for isotachopheresis was prepared, where a mixture of DNA origami and thrombin spiked cell lysate was electrophoresed and concentrated between the loading electrolyte (LE) and the trailing electrolyte (TE). The concentrated fraction of DNA origami-thrombin complex was then extracted from the cross section of the microfluidics chip and confirmed by AFM. Successful thrombin detection from cell lysate spiked with 15 nM thrombin was achieved. Recently, all atom molecular dynamics studies were performed to simulate the binding behaviour of dual thrombin aptamer system with a 1152 nt scaffold small DNA origami structure, 26 nt thrombin aptamer (NU172, also known as ARC2172)[48] and 29 nt-long thrombin aptamer (HD22) [49].

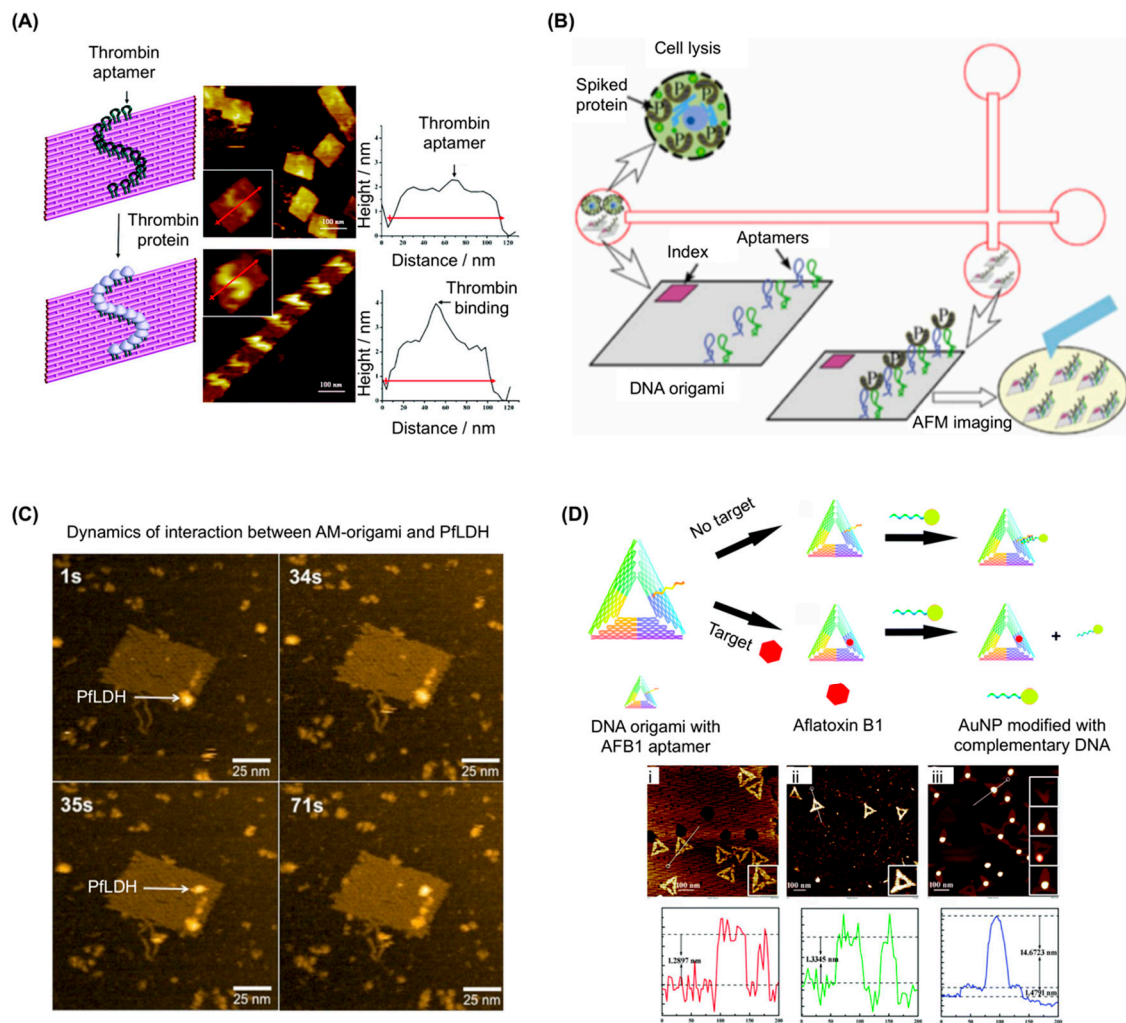


Figure 2. Examples of aptamer use in target immobilization on DNA origami. (A) (left) Schematic showing an S-shaped pattern of thrombin templated on DNA origami. Grey balls represent thrombin proteins. (middle) Images corresponding to the arrays shown on the left, with zoomed-in images (inset); (right) line cross-section analysis of the AFM images show an increase in the height at the sites of protein binding. Adapted with permission from Chhabra et al [20]. Copyright (2007) American Chemical Society. (B) Schematic for stacking, separation and identification of DNA origami and its protein binding using ITP in a cross-channel microfluidic chip fabricated in fused silica. DNA origami with bivalent aptamers was assembled by replacing individual staple strands. Thrombin was used as the target analyte to provide functional validation. After incubating origami in thrombin-spiked cell lysate, separation was performed by on-chip ITP and verified by direct visualization with atomic force microscopy (AFM). Adapted with permission from Mei et al, *Nano Res.*, 2013 [47]. (C) HS-AFM images showing dynamics of interaction between AM-origami and PflDH. At 1 s, a single AM-origami is visible with one PflDH (indicated by white arrow) attached to the aptamer-modified region. At 35 s a second PflDH (indicated by white arrow) binds to the region and both proteins remain in place beyond 71 s. Adapted from Godonoga et al. [50]. (D) (top) Schematic illustration of the analytical principle of the aptamer-tagged DNA origami/complementary ssDNA-AuNPs system for detecting AFB1; (bottom) AFM images with section plots of aptamer-tagged triangular DNA origami nanostructures before and after binding. (i) Aptamer-tagged triangular DNA origami; (ii) aptamer-tagged triangular DNA origami after binding with AFB1; (iii) aptamer-tagged triangular DNA origami after hybridization with the

AuNP-conjugated ssDNA. From Lu et al, Chem. Commun., 2017 [51] – Reproduced by permission of The Royal Society of Chemistry.

Rothemund's rectangular DNA origami structure has been utilised by several groups as a basis for pegboard biosensor construction. For example, dual thrombin aptamers (HD1 and HD22), inactivated by an O⁶-methyl modification of guanine base in advance, have been used to detect the activity of the DNA repair enzyme, human O⁶-alkylguanine-DNA alkyltransferase (hAGT)[52]. When the sample mixed with the biosensor has demethylation activity, the original sequence of the thrombin aptamer is recovered and it will immobilise thrombin on DNA origami, which is visible in AFM. As inhibition of hAGT can enhance the cytotoxicity of alkylating agents in tumour cells, this system has potential use in screening inhibitors as candidate chemotherapy enhancers. In another example[50] we developed a DNA origami biosensor with potential for malaria detection by integrating recently discovered *Plasmodium falciparum* lactate dehydrogenase (PfLDH) aptamers (2008s) (Figure 2C)[53] which are notable as PfLDH is a biomarker of malaria infection. Twelve PfLDH aptamers were arrayed on a DNA rectangle via 20 nt poly T linkers and specific binding of PfLDH was observed using AFM and high-speed AFM (HS-AFM) measurements. Although the affinity was decreased when the aptamer was connected to staple strands (Native $K_D \sim 56 \pm 18$ nM, staple connected: $K_D \sim 600$ -1100 nM), the aptamer modified DNA rectangle selectively captured PfLDH at concentrations as low as 500 nM and functioned even in presence of blood plasma. Captured PfLDH retained enzymatic activity allowing biochemical detection using methods other than AFM imaging. Others have constructed a DNAzyme-operated logic gate system able to release a detectable analyte only in the presence of certain DNA strands[54]. In these conditions, a DNA sequence on the DNA origami surface was cleaved by a DNAzyme, leading to ssDNA release. The released DNA could be pre-labelled with detectable moieties such as ruthenium dye and gold nanoparticles (AuNP). Protein capture and programmed release was demonstrated by incorporating the thrombin aptamer (HD1) into the cleavable strand[54] with released thrombin being detectable e.g. via SDS PAGE.

A NOT gate was constructed on a triangular DNA origami structure to detect the small molecule, aflatoxin B1 (AFB1), using the pegboard based detection method (Figure 2D) [51]. Here staple strands were modified with a AFB1-binding aptamer[55] sequence. In the absence of AFB1, a complementary sequence with a AuNP attached was able to hybridise to the aptamer, detectable via AFM and gel electrophoresis. If AFB1 is present, it is bound by the aptamer meaning that the gold-labelled strand cannot bind. This NOT gate system enables detection of a small molecule target that is not visible in AFM. Other alternatives to microscope imaging-based methods for detecting binding to aptamers on origami have been demonstrated with one example using surface plasmon resonance to evaluate the interaction of 3D DNA origami structure with thrombin aptamer (HD22) and thrombin and optimise detection[56].

Since aptamers can precisely localise proteins onto the surface of DNA origami, we foresee that this will be a useful approach for biophysical characterisation of enzymes and for nanoreactors. Similar ideas have been demonstrated using protein-DNA conjugates on various designs of origami. For example, glucose peroxidase and horseradish peroxidase have been physically coupled through origami for peroxidation of ABTS or TMB resulting in signal generation, as reviewed in 2017 [57]. Since DNA origami is highly programmable, the functionalisation of this enzyme cascade could be optimized through varying the spacing distance between enzymes, thereby providing insight into mechanism [58].

As aptamers can be defined as single-stranded nucleic acids binding specifically to a target, known sequences which bind to a specific protein could also be regarded as aptamers. The Morii group has developed Zinc-finger [59] or leucine-zipper [60] based DNA binding motifs to array target proteins on DNA nanostructures. In 2016, they created an artificial enzyme cascade by incorporating binding sites for xylose reductase and xylitol dehydrogenase at specific locations on DNA origami [61]. Both binding sites were single stranded DNA and one of them had a benzylguanine modification on thymine for binding to xylitol dehydrogenase. This design of origami resembled the xylose metabolic pathway. Enzymatic activity resulting in generation of xylulose and NADH could also be

controlled through modulating inter-enzyme distances. Recent work from the same group also demonstrated the use of zinc-finger protein adaptors consisting of single-stranded hairpin structures for the binding of Kir3 K⁺ channel proteins [62]. The precise fabrication allowed design of various cavities in the DNA origami such that K⁺ channel current activity could be controlled by the oligomerization state of the protein complex. With more aptamers being developed against different targets, such approaches point towards particular promise for aptamers integrating with DNA origami potentially having the ability to modulate membrane protein activity.

In summary, DNA origami has expanded the concept of protein nanoarrays which was formerly investigated only on relatively smaller DNA nanostructures. Combining AFM visualisation and simple logic gates, a series of biosensor devices have been proposed targeting thrombin, PDGF, hAGT activity, PflDH and AFB1. Challenges include the fact that integration of aptamers into DNA nanostructures may suppress the affinity for target due for example, to the sequence extensions required for connection to the larger structure, imperfect DNA origami assembly and steric hindrance for target molecule which can be partially recovered by optimising aptamer positioning and linker length. Combining simple logic gates with aptamers enables detection of aptamers targeting small particles which may be too small to be easily detectable in AFM imaging. A summary of aptamers used in conjunction with DNA origami are given in Table 1.

Table 1. Summary of aptamer utilised in DNA origami research

Name	Target	Sequences	Length / DNA or RNA	Employ ed by	Re f
HD1	Thromb in (exosite I)	GGTTGGTGTGGTTGG	15nt ssDNA	[46, 47, 52, 54]	[3]
HD22	Thromb in (exosite II)	AGTCCGTGGTAGGGCAGGTTGGGGTGACT	29nt ssDNA	[17, 49, 52, 56]	[45]
NU172 (former name: ARC2172)	Thromb in	CGCCTAGGTTGGGTAGGGTGGTGCG	26nt ssDNA	[49]	[48]
36t	PDGF	CACAGGCTACGGCACGTAGAGCATCACCATGATCCTGTGT	40nt ssDNA	[17]	[44]
41t	PDGF	TACTCAGGGCACTGCAAGCAATTGTGGTCCCAATGGGCTGA GTAT	45nt ssDNA	[63-65]	[44]
SL12	VEGF	ATACCAGTCTATTCAATTGGGCCCCGTCCGTATGGTGGGTGTG CT 45-66 sequence was truncated.	44nt ssDNA	[65]	[66]
TE17	CCRF- CEM cell	CAGCTACGCAATACAAAACCTCCGAACACCTGCTTCTGACTG GGTGCTG	48nt ssDNA	[63]	[67]
sgc8c	PTK7	ATCTAACTGCTGCGCCGCCGGGAAAATACTGTACGGTTAGA	41nt ssDNA	[63]	[68 , 69]
2008s	PflDH	CTGGGCGGTAGAACCATAGTGACCCAGCCGTCTAC	35nt ssDNA	[50, 70]	[53]
AFB1 aptamer	AFB1	GTTGGGCACGTGTTGTCTCTGTGTCTCGTGCCCTTCGCTAG GCCCCAC	49nt ssDNA	[51]	[55]

ATP aptamer	ATP	ACCTGGGGGAGTATTGCGGAGGAAGGT In [71, 72], single G at 3' end was added as a result of optimisation.	27nt ssDNA	[71-73]	[74, 75]
ATP aptamer	ATP	1: CTAcUACCTGGGGGAGTAT 2: TGCGGAGGAAGGTcUAG cU is dye modified nucleoside.	43nt ssDNA	[76]	[77]
aptakiss and GTP switch	GTP	aptakiss: UGCUCGGCCCCGCGAGCA GTPswitch: UCCGAAGUGGUUGGGCUGGGGCGUGUGAAAACGGA GTPswitch mutant: UCCGAAGUGGUUGGGCUGGGGCGUGUGAAAACGGA	18nt RNA/35 nt RNA	[78]	[79]
S2.2	MUC-1	GCAGTTGATCCTTTGGATACCCTGG	25nt ssDNA	[80, 81]	[82]
cocaine aptamer	cocaine	GGGAGACAAGGATAAATCCTTCAATGAAGTGGGTCTCCC Derivative of MNS-4.1[83]	39nt ssDNA	[72, 73]	[84]
AS1411 (former name: AGRO100)	Nucleolin	GGTGGTGGTGGTTGTGGTGGTGGTGG	26nt ssDNA	[85]	[86, 87]
C2NP	CD30	ACTGGGCGAAACAAGTCTATTGACTATGAGC	32nt ssDNA	[88]	[89]
zif268 binding site	zif268	CTGCGTGGGCGTGTTTTACGCCCACGCAG	30nt ssDNA	[57, 59, 62]	[59]
AZP4 binding site	AZP4	CTTACGTGGCATGTTTCATGCCTCGTAAG	29nt ssDNA	[59, 62]	[59]
GCN4 binding site	GCN4	CTTCATGAGTCATGCGTTTTTCGCATGACTCATGAAG	36nt ssDNA	[57, 60]	[60]

3. Aptamers for controlling DNA origami structural changes

Molecular recognition by aptamers is accompanied by conformational change. By optimising the equilibrium between the partially complementary strand hybridisation and target-aptamer binding, aptamers behave as a molecular switches, converting the detection of specific target molecule into structural change of DNA, which can be further converted to detectable outputs such as fluorescence signal shifts (Figure 3A)[90]. If such aptamer modules are included in DNA nanostructures, aptamer-target interaction can be made such that it results in release of the strand complementary to the aptamer strand, leading to dynamic transformation of the overall structure (Figure 3B). Where aptamers already consist of two moieties[79] or have been split by design[91], they can be reconstituted into a single complex in presence of target molecule. When each moiety of such an aptamer module is integrated to a distal site on the DNA nanostructure, molecular recognition brings the two parts together. In this way, aptamers can be used to actuate motion in DNA origami systems in response to specific molecular signals and different aptamers in parallel can be used to instantiate logic gates. To date, a number of DNA origami structures have demonstrated the use of aptamers in this way as described below.

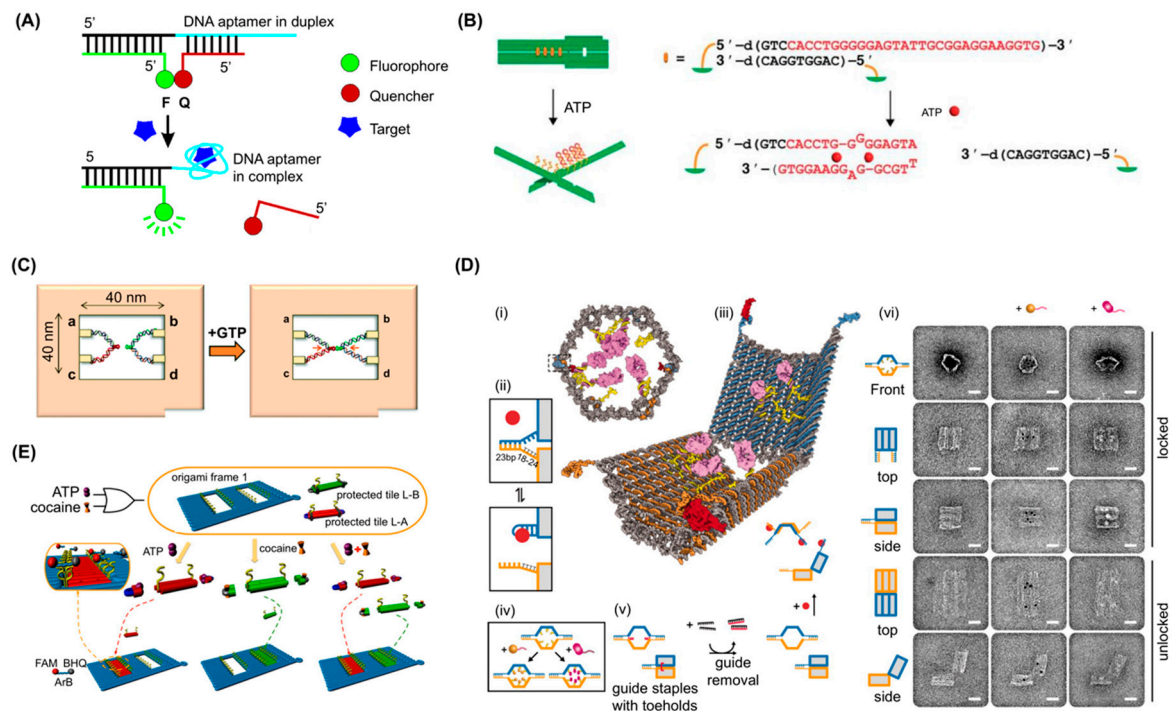


Figure 3. Examples of aptamer use in controlling DNA origami structural change. (A) Schematic for designing aptamer-based fluorescent reporters that function by switching structures from DNA/DNA duplex to DNA/target complex. Adapted with permission from Nutiu et al [90]. Copyright (2003) American Chemical Society. (B) Key and lock system to detect ATP using aptamer-based elements. Adapted from Kuzuya et al [71]. (C) Schematic of the system for investigating the interaction of kissing RNA aptamers using a DNA frame. Incorporation of the aptakiss into the a–c site and KG51 or GTPswitch into the b–d site in the DNA frame. When the GTPswitch is incorporated into the DNA frame, GTP should induce conformational change from the double-loop to the X-shape. From Takeuchi et al, [78] – Reproduced by permission of The Royal Society of Chemistry. (D) (i) Schematic of the front view of a closed nanorobot loaded with a protein payload; (ii) the DNA aptamer (blue) and a partially complementary strand (orange) make the aptamer lock. The lock can be stabilized in a dissociated state by its antigen key (red); (iii) mechanism of nanorobot opened by protein displacement of aptamer locks. The two domains (blue and orange) are constrained in the rear by scaffold hinges; (iv) Payloads (gold) and antibody Fab' fragments (magenta) can be loaded inside the nanorobot; (v) Front and side views show guide staples (red) bearing 8-base toe-holds that aid assembly of the nanorobot. After folding, guide staples are removed by addition of fully complementary oligos (black). Nanorobots can be subsequently activated by interaction with antigen keys (red); (vi) TEM images of robots in closed and open conformations. From Douglas et al [63]. Reprinted with permission from the American Association for the Advancement of Science. (E) Schematic illustration of the “OR” gate using ATP and cocaine as two independent inputs to trigger the filling patterns. In the locking step, both tile A or B can be deactivated by hybridizing with the protector strands PA or PB, which contain aptamer-recognizing sequences of ATP and cocaine in the middle region, respectively. In the unlocking step, the protector strands (PA or PB) at the ends of the L-A or L-B can be removed by adding the aptamer target (ATP or cocaine). Adapted with permission from Yang et al [73]. Copyright (2016) American Chemical Society.

225 3.1. DNA origami functionalized with potential as biosensors

226 A biosensor oriented nanomechanical DNA origami structure was initially reported in 2011
 227 (Figure 3B)[71]. This design consisted of a pliers-shaped or scissors-shaped DNA origami
 228 nanostructure of two DNA origami bars covalently connected at their two centres by single

crossovers and one to four pairs of sensory modules including ATP aptamers[74, 75]. The aptamer and its complementary strands formed four pairs of “aptamer locks” to convert the DNA nano-pliers from an open X-shape to a closed parallel bar shape. In presence of 1 mM ATP, mimicking cellular concentrations, the aptamer module captures ATP, releasing the complementary strand, resulting in a decrease of the fraction of closed form DNA pliers from 72% to 40%. Target specificity was confirmed using GTP as negative control. One to four pairs of telomere elements were also integrated, these dimerize and form a G-quadruplex in the presence of sodium (or potassium) ions. The modules acted as a zipper to close the DNA nanostructure from X form to parallel form in the presence of sodium or potassium ions. Thus, the dynamic DNA origami structure converted binding of small ligand to target aptamer mechanical transformation (opening or closing) of a large DNA origami measurable by AFM imaging at a single molecular level or via a real-time fluorescence spectrum shift of fluorescence resonance energy transfer (FRET) in bulk.

A mechanochemical DNA origami device utilising a PDGF aptamer was demonstrated in 2014[64]. In this approach, a 7-tile DNA origami nanostructure was designed in which the recognition elements interlock adjacent tiles. The binding of a target to any of the recognition elements releases the lock, which generates a change in mechanical force signal, constantly measured by optical tweezers. A PDGF aptamer[44] was used as the first recognition element in each of the six interlocks. The detection sensitivity of the 7-tile origami device was as low as 10 pM within 10 min, improving from 100 pM within 30 min[92] for a former single-interlock system, implying the arrangement of multiple sensor units in series enhanced both the detection limit as well as detection time. A multiplexing capacity of the platform by integrating a pair of DNA hybridisation locks with toehold sequence and an aptamer lock together into the same device simultaneously was also demonstrated[93]. DNA origami and aptamers have been combined to observe RNA kissing complex formation with single molecule resolution [78]. To do this, a frame-shaped DNA origami structure was designed with the two RNA sequences on opposite sides of a central hole. One sequence was a designed aptamer motif (GTPswitch) which binds to the other moiety (aptakiss) responding to the presence of GTP [79]. Before addition of GTP, both aptamers were visible in AFM as discrete structures, forming a double loop shape. This became an X-shape after the addition of GTP (Figure 3C) [78]. The GTPswitch sequence was optimised to attain a statistically significant detection of 1 mM GTP ($65.2 \pm 0.5\%$ from $44.0 \pm 2.0\%$ in absence of target molecule) and discrimination against ATP ($46.4 \pm 2.5\%$ X-shape in presence of 1 mM ATP) meaning that GTP detection at a single molecule level was achieved.

As DNA origami is modular methodology, many groups have introduced various aptamers into established structures for further functionalisation. For example, a split aptamer able to bind two molecules of ATP [77] was introduced into the nanomechanical DNA origami pliers[76]. The aptamers were labelled with different dyes such that a FRET fluorescence spectrum shift would occur if the dyes approached each other (i.e. if the pliers closed). In the presence of 0.1 mM to 1 mM ATP, the split aptamers bound ATP, reconstituting the native aptamer and closing the DNA pliers resulting in successful detection of ATP by FRET in real-time, confirmed by AFM and agarose gel electrophoresis. Aptamers may have a use in targeting DNA origamis to cancer cells and a set of aptamers for cancer-specific Mucin 1 protein (MUC-1) [82] have been integrated into a spherical DNA origami structure[94]. In the system, two hemispheres are connected by single crossover and five pairs of ssDNA evenly protrude from equatorial helices of both hemispheres. After assembling the opened structure, each pair of the ssDNA overhangs are interlocked by lock strands containing a centrally positioned MUC-1 aptamer sequence. In presence of the “key”, i.e. the target protein or the complementary strand for the lock strands, the lock strands are removed from the DNA nanostructure, leading to opening of the sphere. The device was demonstrated as opening on exposure to MUC-1-containing cell lysate[81]. Other aptamers used in relation to disease treatment or detection include the PflDH aptamer[53] which has been shown to work as part of a malaria biosensor/prototype therapeutic delivery system whereby the aptamers control the opening of a DNA origami box.[70] In this work two pairs of aptamer lock with partially complementary strands were integrated between the lid and main box. The conformational change of the PflDH aptamer on

binding PflDH competes with the duplex formation closing the box lid. In absence of the target molecule or presence of negative control (human LDH-B), the boxes with aptamer locks showed mostly closed conformation (20% of DNA box open according to TEM imaging) while in presence of 100 nM PflDH, DNA box opened reaching ca 70% in the open form during 120 min of incubation. Opening of the box by FRET based kinetics was also monitored. Due to the complementary strands locking the lid, the estimated K_D of the aptamer was 655 nM, weaker than native aptamer with K_D of approx. 42 nM.

3.2 DNA origami for Molecular Computing

Production of programmable DNA origami machines is a major goal. Indeed, many of the aptamer -operated origami structures to date respond only if aptamer binds to signal and so could be said to be a form of Boolean logic gate. However, beyond the largely sensory modules described above, aptamer integration has offered more sophisticated programmability to DNA origami structures[31, 32, 95].

One of the most innovative examples was demonstrated in 2012[63]. Here, a capsule-shaped structure with two pairs of different aptamer locks closing the shape was designed (Figure 3D) and a PDGF aptamer (41t)[44], protein kinase 7 aptamer (Sgc8c)[68, 69] and CCRF-CEM cell targeting aptamer (TE17)[67] used. A cargo of up to 12 antibody (fragments) were encapsulated to target the nanorobot to specific cells displaying antigen receptors, enabling the DNA origami structure to discriminate cell types amongst Burkitt's lymphoma, acute myeloblastic leukemia, aggressive NK leukemia, T-cell leukemia, acute lymphoblastic leukemia and neuroblastoma. Cells not expressing the molecular "keys" to open the aptamer locks were not bound by the loaded DNA origamis, while cells expressing the keys were, due to opening of the structure and exposure of the antibody fragments. By using two different aptamer locks on a single DNA origami structure, an AND gate could be constructed whereby the capsule would open only in the presence of both molecular keys. Due to fluorescence labelling of the antibody fragments, the binding of DNA origami to target cell types could be verified verified by FACS [63]. It is interesting to note that a high yield of closed DNA origami structures was obtained by using additional "guide" staple strands to help set the closed state. These could subsequently be removed prior to interaction with target. In this way a yield of 97.5% of closed conformation was achieved.

The logic gate system, was subsequently expanded to include more sophisticated programmability ex-vivo as well as in vivo using a cockroach model [65]. A barrel-shaped encapsulating DNA origami structure similar to that described above was designed and PDGF aptamer (41t) and vascular endothelial growth factor (VEGF) aptamer (SE12) [66] locks were used to produce an effector robot (E) with an AND gate. Then a positive regulator (P) DNA origami was constructed, which was loaded with ssDNA complementary to one of the locking strands of the effector such that binding of the two robots opens E regardless of aptamer-ligand interaction. Similarly, a negative regulator (N) was constructed which carries two ssDNAs complementary to two locks on opposite sides of E, keeping it closed regardless of aptamer-ligand interaction. With a different toehold sequence present on the locking strands, a secondary effector robot (F), which is sensitive to PDGF and VEGF but is not activated or inactivated by positive or negative regulators, was also introduced. Combining P, N and F robot in addition to the original nanorobot with an AND gate behaviour resulted in successful emulation of AND, OR, XOR, NAND, NOT, CNOT and half adder logic-gates.

Other logic-gate systems have been implemented in DNA origami to detect molecules of interest. For example a DNA origami frame was produced containing two holes which could be filled by DNA tiles in the presence of predefined target molecules, in this case ATP and cocaine (Figure 3E) [73]. The DNA tile modules are inactivated by aptamer-locks[83, 84] which prevent them from filling the holes, but in the presence of ATP or cocaine, the aptamer locks are released from the DNA tiles activating sticky ends that have complementarity to sequences lining the holes. Whether the holes are unfilled or filled can be detected by AFM. In this system the design elegantly included a mechanism whereby detection could be achieved without requiring AFM. To do this a DNazyme (Mg^{2+} -dependent E6-

type DNAzyme-1) was reconstituted when the tiles bound into the holes. The reconstituted DNAzyme cleaved a fluorescent reporter which included a fluorophore and quencher such that active DNAzyme resulted in an increase in fluorescent signal. Combinations of these reporter systems enabled emulation of OR, YES and AND logic gates using ATP and cocaine as input signals.

A second ATP/cocaine aptamer based logic gate nano-system[72] has been demonstrated which utilises hexagonal DNA nanostructures [96] that can connect to each other laterally via aptamer locks. four pairs of aptamer locks were embedded to connect two hexagonal DNA origami structures via side-by-side dimerization and dissociation of the structure was optimised. As a result, the yield for the dimeric form of the structure reached 89% which was decreased to 24% in presence of 5 mM ATP in 2 hr. Similarly, the cocaine aptamer lock was used to mediate dimerization with dimer constituting 87% and 33% of the total in the absence or presence of 5 mM cocaine respectively. Finally, combining the two aptamer locks formed a DNA origami trimer. Each DNA origami monomer was labelled by 0 to 2 streptavidin flags to distinguish them. The trimer was designed to dissociate into dimer and monomer in presence of either ATP or cocaine or to dissociate into monomer in presence of both signals. The DNA origami trimer was produced with 80% yield, which decreased to 19% in the presence of either ATP or cocaine and to 2.8% in presence of both signals. The dimeric form (approx. 40%) observed in presence of either signal clearly demonstrated controlled dissociation with low crosstalk

Overall, aptamer locks and split aptamers offer the capability for dynamic transformation of DNA origami structures that can produce a response as a result of target molecule recognition. As a biomarker device, the detection of target molecules such as ATP, Na⁺, K⁺, GTP, PDGF, cocaine and PflDH have been converted to dynamic transformations of DNA origami structures, as evaluated by AFM or TEM, optical tweezers, as well as agarose gel electrophoresis or tracked real-time by fluorescence signal alteration, derived from FRET or quenchers. As each DNA nanostructure can possess more than one aptamer module, AND gates can be easily constructed by integrating orthogonal aptamer modules. Designing sequential reactions of DNA origami structure interactions, allows various kinds of logic gate to be demonstrated. In all cases, high efficiency of transformation control is challenging. Aptamer sequence themselves, along with complementary sequences and the position and multivalency of aptamer modules need to be further optimised for improved performance.

4. Aptamers for Cell Targeting

Analogously to their protein antibody counterparts, DNA aptamers have been developed which bind to specific receptors that are displayed on the surface of certain cell types (e.g. cancer cells)[97]. In some cases, aptamers binding to these receptors can promote uptake of the conjugated structures by the cell as well as triggering cellular signals. This has been utilised in a number of cases to target DNA nanostructures to specific cells with therapeutic goals, as has recently reviewed by Kim et al. including a useful table of cell selectivity of aptamers [98]. Sgc8c, also used in the programmable DNA origami robot mentioned above,[63] targets protein tyrosine kinase 7 (PTK7), a transmembrane receptor highly expressed in cancer cell lines including T-cell acute lymphoblastic leukemia[69]. The MUC-1 aptamer, S2.2, also used in the DNA nanosphere work[81], targets MUC-1 receptor positive cancer cell lines including MCF-7 breast cancer cells[82]. AS1411 is a popular aptamer targeting the nucleolin receptor, which is displayed on rapidly proliferating cells including various cancer cells [86, 87]. These cell targeting aptamers are widely employed to functionalise DNA nanostructures such as an icosahedral DNA nanostructure [99] or ring-shaped DNA nanostructure[100], both with 12-valent S2.2 decoration to deliver doxorubicin (Dox, dsDNA intercalating anti-cancer drug); A long linear DNA nanostructure with a Sgc8c or an AS1411 motif to deliver Dox [101]; a fluorophore labelled dendric DNA nanostructure with Sgc8c to specifically deliver Dox to cancer cells in vitro[102]; Y or X shaped DNA nanostructures with Sgc8c, TC01 (aptamer targeting) and Sgc4f[103]; a tetrahedral DNA nanostructure with trivalent AS1411 which reduces growth of cancer cells [104]; and another DNA tetrahedron with both AS1411 and MUC-1 aptamers delivering Dox [105] along with many others[106, 107].

It is noteworthy that nanoparticles in a certain size range are passively accumulated to solid cancer tumours by the enhanced permeability and retention (EPR) effect and then are taken in to cells by endocytosis [108], this is encouraging for DNA nanoscience as DNA origami structures are typically within this size range. So far a 30 helix bundle (HB) DNA origami tube decorated with 62-valent CpG motif for TLR9 mediated immune response[26]; 6HB tubular or triangular DNA origami structures carrying Dox[109], a twisted DNA origami tube with tuneable Dox capacity and releasing rate[110] and a 26HB rod-like DNA origami structure carrying daunorubicin [111] have been used to take advantage of this effect. A systematic comparison of cellular uptake efficiency among DNA nanostructures and 3D DNA origami structures with gold nanoparticles (AuNP) [112] have shown in vitro cell uptake of DNA origami structures, while in vivo passive accumulation and cellular intake of various shapes of naked DNA origami structures carrying Dox [113] or gold nanorod (AuNR)[114] as well as lipid membranes and PEG coated octahedral DNA origami structures [115] have been demonstrated.

Passive DNA origami delivery with Dox[109] or AuNRs [114], integrated with MUC-1 aptamer (S2.2) to enhance cell targeting of a triangular DNA origami structure has been reported, where the structure carries both Dox and AuNR as anticancer drugs (Figure 4A) [80]. AuNR synergistically suppressed the expression of P-glycoprotein and the growth of multidrug resistant MCF-7 cells upon NIR irradiation via the hyperthermia effect [116] and the work successfully demonstrated an aptamer derived cell intake enhancement of the DNA origami structure. Further development allowed attachment of two capped p53 gene modules to the triangular DNA origami carrying Dox, designed to be released and expressed after delivery into the cells, which was tested and showed efficacy in mice[117]. Another report utilised the C2NP aptamer, which recognises CD30 positive cancer cells including K299 and triggers a signalling pathway leading to apoptosis at high concentration[89]. S DNA rectangle decorated with four or sixteen such aptamers enhanced cell specific Dox delivery and apoptosis induction[88].

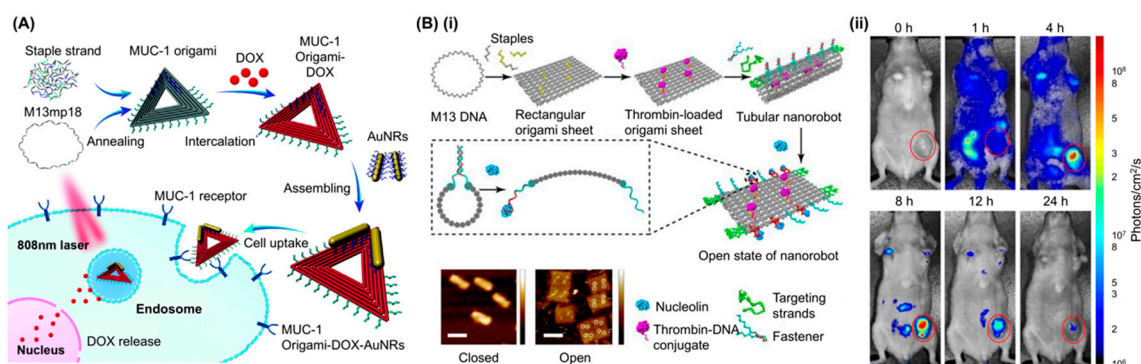


Figure 4. Examples of aptamer use in cell targeting of DNA origami. (A) Schematic showing that triangle DNA origami functionalized with the MUC-1 aptamer can load doxorubicin and carry AuNRs to inhibit the growth of resistant breast cancer cells. Triangular shaped DNA origami structure is hybridized with staple strands (grey), MUC-1 aptamer strands (green) and capture strands (blue). The multifunctional DNA nanostructures (MUC-1 aptamer-DNA origami-DOX-AuNRs complex, MODA) were administered to the MCF-7/ADR cells, and the photothermal effects were investigated. Adapted with permission from Song et al, Nanoscale, 2017 [80]. **(B) (i)** (top) Schematic showing of the construction of thrombin-loaded nanorobot by DNA origami, and its reconfiguration into a rectangular DNA sheet in response to nucleolin binding. (bottom) AFM images of the DNA nanorobots in closed (left) and opened states (right). The four bright spots displayed on the surface of the origami sheet represent the thrombin molecules. **(ii)** In vivo experiment to show the activity of aptamer-based DNA nanorobots. Optical imaging of an MDA-MB-231 mouse bearing a human breast tumor before and after intravenous injection of Cy5.5-labeled nanorobot. A high-intensity fluorescent signal was detected only in the tumor region of

mice 8 h after injection. 0 h indicates before injection. Adapted with permission from Li et al, Nat. Biotechnol., 2018 [85].

Recently, an intelligent DNA origami nanorobot, that can target tumours in mice, inhibiting their growth, has been reported (Figure 4B)[85]. In the design, the authors employed AS1411 not only for targeting cancer cells, but also to regulate the mechanical transformation of the DNA nanorobot to expose the cargo at the focus. They first loaded bioactive thrombin-DNA conjugates to four positions of the same surface of a rectangular DNA origami structure by hybridisation. Then the DNA structure was rolled and “fastened” by six pairs of AS1411 aptamer locks to form a hollow tube. The locks are opened upon interaction with nucleolin. The nanorobot was further decorated with eight AS1411 strands to enhance cell targeting. Thrombin was kept inside the hollow structure to protect it from the innate coagulation system during delivery and was exposed to surrounding only when the nanorobot reached nucleolin positive cells, causing a coagulation cascade that eventually induces necrosis of tumour tissue. Using MDA-MB-231 model mice bearing a human breast cancer tumour as well as C57BL/6J mice injected with B16-F10 melanoma tumour cells, they successfully demonstrated cancer tissue targeting, designed necrosis, tumour growth inhibition and enhancement of survival time.

Conclusion and Perspective

In this review we have summarised the various examples wherein DNA aptamers have been combined with DNA origami and noted that the work can be separated into four distinct areas. In the first, aptamers are used as protein immobilisation modules capable of capturing and arranging proteins in defined patterns and with defined order. This may even allow control and manipulation of protein to produce designed protein-based nanomachines but on a DNA origami framework. The second and the third areas show how aptamers can be used to initiate and control structural changes in DNA origami, allowing extremely sensitive detection and linking the output of molecular logic gates to conformational dynamism. Finally, cell targeting aptamers enable specificity of drug delivery by DNA origami carriers. As listed in Table 1, the majority of the research relies on a limited number of established aptamers to demonstrate feasibility of designs while some have utilised DNA origami to expand the applications of newly developed aptamers[50, 70, 76, 78]. There are more aptamers, both well-characterised or novel that are potentially useful for functionalisation of DNA origami structures with various potential applications. Some have already been used in DNA nanostructure research or other bioconjugate research reviewed elsewhere [4, 12, 38, 104]. As demonstrated by the work replacing an ATP aptamer lock with a new split aptamer system to enhance efficiency of DNA origami device transformation [71, 76], seeking alternative aptamers could overcome a general problem, which is that the aptamer affinity generally decreases upon attachment to DNA origami. This is likely due to steric and electrostatic effects. An intelligent DNA nanorobot with AS1411 for both cell targeting and drug release[85] exemplifies the new possibility of development of sophisticated DNA origami devices utilising multiple aptamers simultaneously to achieve synergistic effects or programmability and we hope that this brief review encourages and further development of improved aptamers for integration with DNA origami.

Author Contributions: JGH conceived and supervised writing of the paper. JGH, YS, MSI, AM, SCCS and JAT all contributed to writing the paper.

Funding: JGH and MSI were funded by the Team Programme of the Foundation for Polish Science co-financed by the European Union under the European Regional Development Fund (TEAM/2016-3/23) awarded to JGH. YS and MA were supported by POLONEZ3 (2016/23/P/NZ1/04097) of Polish National Science Centre (NCN) co-funded by the Marie Skłodowska-Curie action of the European Union (665778). SCCS and JAT have been funded by grants from the General Research Fund (17119814) of the Hong Kong University Grants Council.

Conflicts of Interest: The authors declare no conflict of interest. The funders had no role in the design of the study; in the collection, analyses, or interpretation of data; in the writing of the manuscript, or in the decision to publish the results.

References

1. Ellington, A. D.; Szostak, J. W., In vitro selection of RNA molecules that bind specific ligands. *Nature* **1990**, 346, (6287), 818-822.
2. Tuerk, C.; Gold, L., Systematic evolution of ligands by exponential enrichment: RNA ligands to bacteriophage T4 DNA polymerase. *Science* **1990**, 249, (4968), 505-510.
3. Bock, L. C.; Griffin, L. C.; Latham, J. A.; Vermaas, E. H.; Toole, J. J., Selection of single-stranded DNA molecules that bind and inhibit human thrombin. *Nature* **1992**, 355, (6360), 564-566.
4. Zhu, Q.; Liu, G.; Kai, M., DNA Aptamers in the Diagnosis and Treatment of Human Diseases. *Molecules* **2015**, 20, (12), 20979-20997.
5. Morita, Y.; Leslie, M.; Kameyama, H.; Volk, D.; Tanaka, T., Aptamer Therapeutics in Cancer: Current and Future. *Cancers* **2018**, 10, (3), 80-22.
6. Pieken, W. A.; Olsen, D. B.; Benseler, F.; Aurup, H.; Eckstein, F., Kinetic characterization of ribonuclease-resistant 2'-modified hammerhead ribozymes. *Science* **1991**, 253, (5017), 314-317.
7. Cummins, L. L.; Owens, S. R.; Risen, L. M.; Lesnik, E. A.; Freier, S. M.; McGee, D.; Guinosso, C. J.; Cook, P. D., Characterization of fully 2'-modified oligoribonucleotide hetero- and homoduplex hybridization and nuclease sensitivity. *Nucleic Acids Res.* **1995**, 23, (11), 2019-2024.
8. Rohloff, J. C.; Gelinas, A. D.; Jarvis, T. C.; Ochsner, U. A.; Schneider, D. J.; Gold, L.; Janjic, N., Nucleic Acid Ligands With Protein-like Side Chains: Modified Aptamers and Their Use as Diagnostic and Therapeutic Agents. *Mol. Ther.* **2014**, 3, (Supplement C), e201.
9. Jarvis, T. C.; Davies, D. R.; Hisaminato, A.; Resnicow, D. I.; Gupta, S.; Waugh, S. M.; Nagabukuro, A.; Wadatsu, T.; Hishigaki, H.; Gawande, B.; Zhang, C.; Wolk, S. K.; Mayfield, W. S.; Nakaishi, Y.; Burgin, A. B.; Stewart, L. J.; Edwards, T. E.; Gelinas, A. D.; Schneider, D. J.; Janjic, N., Non-helical DNA Triplex Forms a Unique Aptamer Scaffold for High Affinity Recognition of Nerve Growth Factor. *Struct.* **2015**, 23, (7), 1293-1304.
10. Ng, E. W. M.; Shima, D. T.; Calias, P.; Cunningham, E. T.; Guyer, D. R.; Adamis, A. P., Pegaptanib, a targeted anti-VEGF aptamer for ocular vascular disease. *Nat. Rev. Drug Discov.* **2006**, 5, (2), 123-132.
11. Kourlas, H.; Schiller, D. S., Pegaptanib sodium for the treatment of neovascular age-related macular degeneration: a review. *Clin. Ther.* **2006**, 28, (1), 36-44.
12. Lao, Y.-H.; Phua, K. K. L.; Leong, K. W., Aptamer Nanomedicine for Cancer Therapeutics: Barriers and Potential for Translation. *ACS Nano* **2015**, 9, (3), 2235-2254.
13. Sundaram, P.; Kurniawan, H.; Byrne, M. E.; Wower, J., Therapeutic RNA aptamers in clinical trials. *Eur. J. Pharm. Sci.* **2013**, 48, (1-2), 259-271.
14. Rothmund, P. W. K., Folding DNA to create nanoscale shapes and patterns. *Nature* **2006**, 440, (7082), 297-302.
15. Wang, P.; Meyer, T. A.; Pan, V.; Dutta, P. K.; Ke, Y., The Beauty and Utility of DNA Origami. *Chem.* **2017**, 2, (3), 359-382.
16. Andersen, E. S.; Dong, M.; Nielsen, M. M.; Jahn, K.; Lind-Thomsen, A.; Mamdouh, W.; Gothelf, K. V.; Besenbacher, F.; Kjems, J., DNA Origami Design of Dolphin-Shaped Structures with Flexible Tails. *ACS Nano* **2008**, 2, (6), 1213-1218.

- 499 17. Chhabra, R.; Sharma, J.; Ke, Y.; Liu, Y.; Rinker, S.; Lindsay, S.; Yan, H., Spatially Addressable
500 Multiprotein Nanoarrays Templated by Aptamer-Tagged DNA Nanoarchitectures. *J. Am.*
501 *Chem. Soc.* **2007**, 129, (34), 10304-10305.
- 502 18. Ke, Y.; Lindsay, S.; Chang, Y.; Liu, Y.; Yan, H., Self-assembled water-soluble nucleic acid
503 probe tiles for label-free RNA hybridization assays. *Science* **2008**, 319, (5860), 180-183.
- 504 19. Williams, B. A. R.; Lund, K.; Liu, Y.; Yan, H.; Chaput, J. C., Self-Assembled Peptide
505 Nanoarrays: An Approach to Studying Protein-Protein Interactions. *Angew. Chem. Int. Ed.*
506 **2007**, 46, (17), 3051-3054.
- 507 20. Sharma, J.; Chhabra, R.; Andersen, C. S.; Gothelf, K. V.; Yan, H.; Liu, Y., Toward reliable gold
508 nanoparticle patterning on self-assembled DNA nanoscaffold. *J. Am. Chem. Soc.* **2008**, 130,
509 (25), 7820-1.
- 510 21. Schnitzbauer, J.; Strauss, M. T.; Schlichthaerle, T.; Schueder, F.; Jungmann, R., Super-
511 resolution microscopy with DNA-PAINT. *Nat. Protoc.* **2017**, 12, (6), 1198-1228.
- 512 22. Steinhauer, C.; Jungmann, R.; Sobey, T. L.; Simmel, F. C.; Tinnefeld, P., DNA Origami as a
513 Nanoscopic Ruler for Super-Resolution Microscopy. *Angew. Chem. Int. Ed.* **2009**, 48, (47), 8870-
514 8873.
- 515 23. Yamazaki, T.; Heddle, J. G.; Kuzuya, A.; Komiyama, M., Orthogonal enzyme arrays on a
516 DNA origami scaffold bearing size-tunable wells. *Nanoscale* **2014**, 6, (15), 9122-5.
- 517 24. Hong, F.; Zhang, F.; Liu, Y.; Yan, H., DNA Origami: Scaffolds for Creating Higher Order
518 Structures. *Chem. Rev.* **2017**, 117, (20), 12584-12640.
- 519 25. Andersen, E. S.; Dong, M.; Nielsen, M. M.; Jahn, K.; Subramani, R.; Mamdouh, W.; Golas, M.
520 M.; Sander, B.; Stark, H.; Cristiano, L. P. O.; Pedersen, J. S.; Birkedal, V.; Besenbacher, F.;
521 Gothelf, K. V.; Kjems, J., Self-assembly of a nanoscale DNA box with a controllable lid. *Nature*
522 **2009**, 459, (7243), 73-76.
- 523 26. Schüller, V. J.; Heidegger, S.; Sandholzer, N.; Nickels, P. C.; Suhartha, N. A.; Endres, S.;
524 Bourquin, C.; Liedl, T., Cellular Immunostimulation by CpG-Sequence-Coated DNA
525 Origami Structures. *ACS Nano* **2011**, 5, (12), 9696-9702.
- 526 27. Kuzyk, A.; Schreiber, R.; Fan, Z.; Pardatscher, G.; Roller, E.-M.; Högele, A.; Simmel, F. C.;
527 Govorov, A. O.; Liedl, T., DNA-based self-assembly of chiral plasmonic nanostructures with
528 tailored optical response. *Nature* **2012**, 483, (7389), 311-314.
- 529 28. Tan, L. H.; Xing, H.; Lu, Y., DNA as a powerful tool for morphology control, spatial
530 positioning, and dynamic assembly of nanoparticles. *Acc. Chem. Res.* **2014**, 47, (6), 1881-1890.
- 531 29. Liu, J.; Lee, J. H.; Lu, Y., Quantum Dot Encoding of Aptamer-Linked Nanostructures for One-
532 Pot Simultaneous Detection of Multiple Analytes. *Anal. Chem.* **2007**, 79, (11), 4120-4125.
- 533 30. Liu, J.; Lu, Y., Smart Nanomaterials Responsive to Multiple Chemical Stimuli with
534 Controllable Cooperativity. *Adv. Mater.* **2006**, 18, (13), 1667-1671.
- 535 31. Mo, R.; Jiang, T.; DiSanto, R.; Tai, W.; Gu, Z., ATP-triggered anticancer drug delivery. *Nat.*
536 *Commun.* **2014**, 5, 1-10.
- 537 32. Liao, W.-C.; Lu, C.-H.; Hartmann, R.; Wang, F.; Sohn, Y. S.; Parak, W. J.; Willner, I., Adenosine
538 Triphosphate-Triggered Release of Macromolecular and Nanoparticle Loads from
539 Aptamer/DNA-Cross-Linked Microcapsules. *ACS Nano* **2015**, 9, (9), 9078-9086.
- 540 33. Yang, F.; Li, Q.; Wang, L.; Zhang, G.-J.; Fan, C., Framework-Nucleic-Acid-Enabled Biosensor
541 Development. *ACS Sens.* **2018**, 3, (5), 903-919.

- 542 34. Li, J.; Green, A. A.; Yan, H.; Fan, C., Engineering nucleic acid structures for programmable
543 molecular circuitry and intracellular biocomputation. *Nat. Rev. Clin. Oncol.* **2017**, 1-12.
- 544 35. Seeman, N. C.; Sleiman, H. F., DNA nanotechnology. *Nat. Rev. Clin. Oncol.* **2017**, 3, (1), 1-23.
- 545 36. Hu, Q.; Li, H.; Wang, L.; Gu, H.; Fan, C., DNA Nanotechnology-Enabled Drug Delivery
546 Systems. *Chem. Rev.* **2018**, acs.chemrev.7b00663-48.
- 547 37. Chen, A.; Yan, M.; Yang, S., Split aptamers and their applications in sandwich aptasensors.
548 *Trends Anal. Chem.* **2016**, 80, (C), 581-593.
- 549 38. Meng, H.-M.; Liu, H.; Kuai, H.; Peng, R.; Mo, L.; Zhang, X.-B., Aptamer-integrated DNA
550 nanostructures for biosensing, bioimaging and cancer therapy. *Chem. Soc. Rev.* **2016**, 45, 2583-
551 2602.
- 552 39. Shiu, S. C.-C.; Kinghorn, A. B.; Sakai, Y.; Cheung, Y.-W.; Heddle, J. G.; Tanner, J. A., The
553 Three S's for Aptamer-Mediated Control of DNA Nanostructure Dynamics: Shape, Self-
554 Complementarity, and Spatial Flexibility. *Chem. BioChem.* **2018**, 17, 437-8.
- 555 40. Alivisatos, A. P.; Johnsson, K. P.; Peng, X.; Wilson, T. E.; Loweth, C. J.; Bruchez, M. P.; Schultz,
556 P. G., Organization of 'nanocrystal molecules' using DNA. *Nature* **1996**, 382, (6592), 609-611.
- 557 41. Yan, H.; Park, S. H.; Finkelstein, G.; Reif, J. H.; LaBean, T. H., DNA-templated self-assembly
558 of protein arrays and highly conductive nanowires. *Science* **2003**, 301, (5641), 1882-1884.
- 559 42. Niemeyer, C. M.; Bürger, W.; Peplies, J., Covalent DNA–Streptavidin Conjugates as Building
560 Blocks for Novel Biometallic Nanostructures. *Angew. Chem. Int. Ed.* **1998**, 37, (16), 2265-2268.
- 561 43. Liu, Y.; Lin, C.; Li, H.; Yan, H., Aptamer-Directed Self-Assembly of Protein Arrays on a DNA
562 Nanostructure. *Angew. Chem. Int. Ed.* **2005**, 44, (28), 4333-4338.
- 563 44. Green, L. S.; Jellinek, D.; Jenison, R.; Ostman, A.; Heldin, C. H.; Janjic, N., Inhibitory DNA
564 ligands to platelet-derived growth factor B-chain. *Biochemistry* **1996**, 35, (45), 14413-14424.
- 565 45. Tasset, D. M.; Kubik, M. F.; Steiner, W., Oligonucleotide inhibitors of human thrombin that
566 bind distinct epitopes. *J. Mol. Biol.* **1997**, 272, (5), 688-698.
- 567 46. Rinker, S.; Ke, Y.; Liu, Y.; Chhabra, R.; Yan, H., Self-assembled DNA nanostructures for
568 distance-dependent multivalent ligand–protein binding. *Nat. Nanotechnol.* **2008**, 3, (7), 418-
569 422.
- 570 47. Mei, Q.; Johnson, R. H.; Wei, X.; Su, F.; Liu, Y.; Kelbaskas, L.; Lindsay, S.; Meldrum, D. R.;
571 Yan, H., On-chip isotachopheresis separation of functional DNA origami capture nanoarrays
572 from cell lysate. *Nano Res.* **2013**, 6, (10), 712-719.
- 573 48. Diener, J. L.; Wagner-Whyte, J.; Fontana, D.; Corp, A., Aptamers that bind thrombin with
574 high affinity. *United States Patent* **2011**, US 7,998,939 B2
- 575 49. Kumar, N.; Seminario, J. M., Molecular dynamics study of thrombin capture by aptamers
576 TBA26 and TBA29 coupled to a DNA origami. *Mol. Simulat.* **2018**, 44, (9), 749-756.
- 577 50. Godonoga, M.; Lin, T.-Y.; Oshima, A.; Sumitomo, K.; Tang, M. S. L.; Cheung, Y.-W.;
578 Kinghorn, A. B.; Dirkzwager, R. M.; Zhou, C.; Kuzuya, A.; Tanner, J. A.; Heddle, J. G., A DNA
579 aptamer recognising a malaria protein biomarker can function as part of a DNA origami
580 assembly. *Sci. Rep.* **2016**, 6, (1), 21266.
- 581 51. Lu, Z.; Wang, Y.; Xu, D.; Pang, L., Aptamer-tagged DNA origami for spatially addressable
582 detection of aflatoxin B1. *Chem. Commun. (Camb.)* **2017**, 53, (5), 941-944.
- 583 52. Tintoré, M.; Gállego, I.; Manning, B.; Eritja, R.; Fàbrega, C., DNA Origami as a DNA Repair
584 Nanosensor at the Single-Molecule Level. *Angew. Chem. Int. Ed.* **2013**, 52, (30), 7747-7750.

- 585 53. Cheung, Y.-W.; Kwok, J.; Law, A. W. L.; Watt, R. M.; Kotaka, M.; Tanner, J. A., Structural
586 basis for discriminatory recognition of Plasmodium lactate dehydrogenase by a DNA
587 aptamer. *Proc. Natl. Acad. Sci.* **2013**, 110, (40), 15967-15972.
- 588 54. Li, F.; Chen, H.; Pan, J.; Cha, T.-G.; Medintz, I. L.; Choi, J. H., A DNzyme-mediated logic
589 gate for programming molecular capture and release on DNA origami. *Chem. Commun.* **2016**,
590 52, (54), 8369-8372.
- 591 55. Le, L. C.; Cruz-Aguado, J. A.; Penner, G. A.; Limited, N. B., DNA ligands for aflatoxin and
592 zearalenone. *United States Patents* **2011**, US 2012/0225494 A1. .
- 593 56. Daems, D.; Pfeifer, W.; Rutten, I.; Saccà, B.; Spasic, D.; Lammertyn, J., Three-Dimensional
594 DNA Origami as Programmable Anchoring Points for Bioreceptors in Fiber Optic Surface
595 Plasmon Resonance Biosensing. *ACS Appl. Mater. Interfaces* **2018**, 10, (28), 23539-23547.
- 596 57. Rajendran, A.; Nakata, E.; Nakano, S.; Morii, T., Nucleic-Acid-Templated Enzyme Cascades.
597 *Chem. Eur. J. of Chem. Bio.* **2017**, 18, (8), 696-716.
- 598 58. Fu, J.; Liu, M.; Liu, Y.; Woodbury, N. W.; Yan, H., Interenzyme Substrate Diffusion for an
599 Enzyme Cascade Organized on Spatially Addressable DNA Nanostructures. *J. Am. Chem.*
600 *Soc.* **2012**, 134, (12), 5516-5519.
- 601 59. Nakata, E.; Liew, F. F.; Uwatoko, C.; Kiyonaka, S.; Mori, Y.; Katsuda, Y.; Endo, M.; Sugiyama,
602 H.; Morii, T., Zinc-Finger Proteins for Site-Specific Protein Positioning on DNA-Origami
603 Structures. *Angew. Chem. Int. Ed.* **2012**, 51, (10), 2421-2424.
- 604 60. Ngo, T. A.; Nakata, E.; Saimura, M.; Kodaki, T.; Morii, T., A protein adaptor to locate a
605 functional protein dimer on molecular switchboard. *Methods* **2014**, 67, (2), 142-150.
- 606 61. Ngo, T. A.; Nakata, E.; Saimura, M.; Morii, T., Spatially Organized Enzymes Drive Cofactor-
607 Coupled Cascade Reactions. *J. Am. Chem. Soc.* **2016**, 138, (9), 3012-3021.
- 608 62. Kurokawa, T.; Kiyonaka, S.; Nakata, E.; Endo, M.; Koyama, S.; Mori, E.; Tran, N. H.; Dinh,
609 H.; Suzuki, Y.; Hidaka, K.; Kawata, M.; Sato, C.; Sugiyama, H.; Morii, T.; Mori, Y., DNA
610 Origami Scaffolds as Templates for Functional Tetrameric Kir3 K⁺ Channels. *Angew. Chem.*
611 *Int. Ed.* **2018**, 57, (10), 2586-2591.
- 612 63. Douglas, S. M.; Bachelet, I.; Church, G. M., A logic-gated nanorobot for targeted transport of
613 molecular payloads. *Science* **2012**, 335, (6070), 831-834.
- 614 64. Koirala, D.; Shrestha, P.; Emura, T.; Hidaka, K.; Mandal, S.; Endo, M.; Sugiyama, H.; Mao, H.,
615 Single-Molecule Mechanochemical Sensing Using DNA Origami Nanostructures. *Angew.*
616 *Chem. Int. Ed.* **2014**, 53, (31), 8137-8141.
- 617 65. Amir, Y.; Ben-Ishay, E.; Levner, D.; Ittah, S.; Abu-Horowitz, A.; Bachelet, I., Universal
618 computing by DNA origami robots in a living animal. *Nat. Nanotechnol.* **2014**, 9, (5), 353-357.
- 619 66. Kaur, H.; Yung, L.-Y. L., Probing High Affinity Sequences of DNA Aptamer against
620 VEGF165. *PLoS ONE* **2012**, 7, (2), e31196-9.
- 621 67. Tang, Z.; Shangguan, D.; Wang, K.; Shi, H.; Sefah, K.; Mallikratchy, P.; Chen, H. W.; Li, Y.;
622 Tan, W., Selection of Aptamers for Molecular Recognition and Characterization of Cancer
623 Cells. *Anal. Chem.* **2007**, 79, (13), 4900-4907.
- 624 68. Shangguan, D.; Tang, Z.; Mallikaratchy, P.; Xiao, Z.; Tan, W., Optimization and Modifications
625 of Aptamers Selected from Live Cancer Cell Lines. *Chem. Eur. J. of Chem. Bio.* **2007**, 8, (6), 603-
626 606.

- 627 69. Shangguan, D.; Cao, Z.; Meng, L.; Mallikaratchy, P.; Sefah, K.; Wang, H.; Li, Y.; Tan, W., Cell-
628 Specific Aptamer Probes for Membrane Protein Elucidation in Cancer Cells. *J. Proteome Res.*
629 **2008**, 7, (5), 2133-2139.
- 630 70. Tang, M. S. L.; Shiu, S. C.-C.; Godonoga, M.; Cheung, Y.-W.; Liang, S.; Dirkzwager, R. M.;
631 Kinghorn, A. B.; Fraser, L. A.; Heddle, J. G.; Tanner, J. A., An aptamer-enabled DNA nanobox
632 for protein sensing. *Nanomed. Nanotechnol.* **2018**, 14, (4), 1161-1168.
- 633 71. Kuzuya, A.; Sakai, Y.; Yamazaki, T.; Xu, Y.; Komiyama, M., Nanomechanical DNA origami
634 'single-molecule beacons' directly imaged by atomic force microscopy. *Nat. Commun.* **2011**, 2,
635 (1), 449.
- 636 72. Wu, N.; Willner, I., Programmed dissociation of dimer and trimer origami structures by
637 aptamer-ligand complexes. *Nanoscale* **2017**, 9, (4), 1416-1422.
- 638 73. Yang, J.; Jiang, S.; Liu, X.; Pan, L.; Zhang, C., Aptamer-Binding Directed DNA Origami
639 Pattern for Logic Gates. *ACS Appl. Mater. Interfaces* **2016**, 8, (49), 34054-34060.
- 640 74. Huizenga, D. E.; Szostak, J. W., A DNA aptamer that binds adenosine and ATP. *Biochemistry*
641 **1995**, 34, (2), 656-665.
- 642 75. Lin, C. H.; Patel, D. J., Structural basis of DNA folding and recognition in an AMP-DNA
643 aptamer complex: distinct architectures but common recognition motifs for DNA and RNA
644 aptamers complexed to AMP. *Chem. Biol.* **1997**, 4, (11), 817-832.
- 645 76. Walter, H.-K.; Bauer, J.; Steinmeyer, J.; Kuzuya, A.; Niemeyer, C. M.; Wagenknecht, H.-A.,
646 "DNA Origami Traffic Lights" with a Split Aptamer Sensor for a Bicolor Fluorescence
647 Readout. *Nano Lett.* **2017**, 17, (4), 2467-2472.
- 648 77. Walter, H.-K.; Bohländer, P. R.; Wagenknecht, H.-A., Development of a Wavelength-Shifting
649 Fluorescent Module for the Adenosine Aptamer Using Photostable Cyanine Dyes.
650 *ChemistryOpen* **2015**, 4, (2), 92-96.
- 651 78. Takeuchi, Y.; Endo, M.; Suzuki, Y.; Hidaka, K.; Durand, G.; Dausse, E.; Toulme, J. J.;
652 Sugiyama, H., Single-molecule observations of RNA-RNA kissing interactions in a DNA
653 nanostructure. *Biomater. Sci.* **2016**, 4, (1), 130-135.
- 654 79. Durand, G.; Lisi, S.; Ravelet, C.; Dausse, E.; Peyrin, E.; Toulmé, J.-J., Riboswitches Based on
655 Kissing Complexes for the Detection of Small Ligands. *Angew. Chem. Int. Ed.* **2014**, 53, (27),
656 6942-6945.
- 657 80. Song, L.; Jiang, Q.; Liu, J.; Li, N.; Liu, Q.; Dai, L.; Gao, Y.; Liu, W.; Liu, D.; Ding, B., DNA
658 origami/gold nanorod hybrid nanostructures for the circumvention of drug resistance.
659 *Nanoscale* **2017**, 9, (23), 7750-7754.
- 660 81. Chaithongyot, S.; Chomanee, N.; Charngkaew, K.; Udomprasert, A.; Kangsamaksin, T.,
661 Aptamer-functionalized DNA nanosphere as a stimuli-responsive nanocarrier. *Mater. Lett.*
662 **2018**, 214, 72-75.
- 663 82. Ferreira, C. S. M.; Matthews, C. S.; Missailidis, S., DNA aptamers that bind to MUC-1 tumour
664 marker: design and characterization of MUC-1-binding single-stranded DNA aptamers.
665 *Tumour Biol.* **2006**, 27, (6), 289-301.
- 666 83. Stojanovic, M. N.; de Prada, P.; Landry, D. W., Aptamer-Based Folding Fluorescent Sensor
667 for Cocaine. *J. Am. Chem. Soc.* **2001**, 123, (21), 4928-4931.
- 668 84. Liu, J.; Lu, Y., Fast Colorimetric Sensing of Adenosine and Cocaine Based on a General Sensor
669 Design Involving Aptamers and Nanoparticles. *Angew. Chem. Int. Ed.* **2006**, 45, (1), 90-94.

- 670 85. Li, S.; Jiang, Q.; Liu, S.; Zhang, Y.; Tian, Y.; Song, C.; Wang, J.; Zou, Y.; Anderson, G. J.; Han,
671 J.-Y.; Chang, Y.; Liu, Y.; Zhang, C.; Chen, L.; Zhou, G.; Nie, G.; Yan, H.; Ding, B.; Zhao, Y., A
672 DNA nanorobot functions as a cancer therapeutic in response to a molecular trigger in vivo.
673 *Nat. Chem.* **2018**, 36, (3), 258-264.
- 674 86. Girvan, A. C.; Teng, Y.; Casson, L. K.; Thomas, S. D.; Jülicher, S.; Ball, M. W.; Klein, J. B.; Pierce,
675 W. M.; Barve, S. S.; Bates, P. J., AGRO100 inhibits activation of nuclear factor-kappaB (NF-
676 kappaB) by forming a complex with NF-kappaB essential modulator (NEMO) and nucleolin.
677 *Mol. Cancer Ther.* **2006**, 5, (7), 1790-1799.
- 678 87. Ireson, C. R.; Kelland, L. R., Discovery and development of anticancer aptamers. *Mol. Cancer*
679 *Ther.* **2006**, 5, (12), 2957-2962.
- 680 88. Sun, P.; Zhang, N.; Tang, Y.; Yang, Y.; Zhou, J.; Zhao, Y., Site-specific anchoring aptamer
681 C2NP on DNA origami nanostructures for cancer treatment. *RSC Adv.* **2018**, 8, (46), 26300-
682 26308.
- 683 89. Parekh, P.; Kamble, S.; Zhao, N.; Zeng, Z.; Portier, B. P.; Zu, Y., Immunotherapy of CD30-
684 expressing lymphoma using a highly stable ssDNA aptamer. *Biomaterials* **2013**, 34, (35), 8909-
685 8917.
- 686 90. Nutiu, R.; Li, Y., Structure-Switching Signaling Aptamers. *J. Am. Chem. Soc.* **2003**, 125, (16),
687 4771-4778.
- 688 91. Stojanovic, M. N.; de Prada, P.; Landry, D. W., Fluorescent Sensors Based on Aptamer Self-
689 Assembly. *J. Am. Chem. Soc.* **2000**, 122, (46), 11547-11548.
- 690 92. Koirala, D.; Yu, Z.; Dhakal, S.; Mao, H., Detection of Single Nucleotide Polymorphism Using
691 Tension-Dependent Stochastic Behavior of a Single-Molecule Template. *J. Am. Chem. Soc.*
692 **2011**, 133, (26), 9988-9991.
- 693 93. Yurke, B.; Turberfield, A. J.; Mills, A. P.; Simmel, F. C.; Neumann, J. L., A DNA-fuelled
694 molecular machine made of DNA. *Nature* **2000**, 406, (6796), 605-608.
- 695 94. Han, D.; Pal, S.; Nangreave, J.; Deng, Z.; Liu, Y.; Yan, H., DNA origami with complex
696 curvatures in three-dimensional space. *Science* **2011**, 332, (6027), 342-346.
- 697 95. Liu, Z.; Tian, C.; Yu, J.; Li, Y.; Jiang, W.; Mao, C., Self-Assembly of Responsive Multilayered
698 DNA Nanocages. *J. Am. Chem. Soc.* **2015**, 137, (5), 1730-1733.
- 699 96. Yang, Y.; Endo, M.; Hidaka, K.; Sugiyama, H., Photo-Controllable DNA Origami
700 Nanostructures Assembling into Predesigned Multiorientational Patterns. *J. Am. Chem. Soc.*
701 **2012**, 134, (51), 20645-20653.
- 702 97. Sefah, K.; Shangguan, D.; Xiong, X.; O'Donoghue, M. B.; Tan, W., Development of DNA
703 aptamers using Cell-SELEX. *Nat. Protoc.* **2010**, 5, (6), 1169-1185.
- 704 98. Kim, M.; Kim, D.-M.; Kim, K.-S.; Jung, W.; Kim, D.-E., Applications of Cancer Cell-Specific
705 Aptamers in Targeted Delivery of Anticancer Therapeutic Agents. *Molecules* **2018**, 23, (4), 830-
706 20.
- 707 99. Chang, M.; Yang, C.-S.; Huang, D.-M., Aptamer-conjugated DNA icosahedral nanoparticles
708 as a carrier of doxorubicin for cancer therapy. *ACS Nano* **2011**, 5, (8), 6156-6163.
- 709 100. Srivithya, V.; Roun, H.; Babu, M. S.; Hyung, P. J.; Ha, P. S., Aptamer-conjugated DNA nano-
710 ring as the carrier of drug molecules. *Nanotechnology* **2018**, 29, (9), 095602.

- 711 101. Zhu, G.; Zheng, J.; Song, E.; Donovan, M.; Zhang, K.; Liu, C.; Tan, W., Self-assembled,
712 aptamer-tethered DNA nanotrains for targeted transport of molecular drugs in cancer
713 theranostics. *Proc. Natl. Acad. Sci.* **2013**, 110, (20), 7998-8003.
- 714 102. Zhang, H.; Ma, Y.; Xie, Y.; An, Y.; Huang, Y.; Zhu, Z.; Yang, C. J., A Controllable Aptamer-
715 Based Self-Assembled DNA Dendrimer for High Affinity Targeting, Bioimaging and Drug
716 Delivery. *Sci. Rep.* **2015**, 1-8.
- 717 103. You, M.; Peng, L.; Shao, N.; Zhang, L.; Qiu, L.; Cui, C.; Tan, W., DNA “Nano-Claw”: Logic-
718 Based Autonomous Cancer Targeting and Therapy. *J. Am. Chem. Soc.* **2014**, 136, (4), 1256-1259.
- 719 104. Charoenphol, P.; Bermudez, H., Aptamer-targeted DNA nanostructures for therapeutic
720 delivery. *Mol. Pharm.* **2014**, 11, (5), 1721-1725.
- 721 105. Liu, X.; Wu, L.; Wang, L.; Jiang, W., A dual-targeting DNA tetrahedron nanocarrier for breast
722 cancer cell imaging and drug delivery. *Talanta* **2018**, 179, 356-363.
- 723 106. Liu, J.; Wei, T.; Zhao, J.; Huang, Y.; Deng, H.; Kumar, A.; Wang, C.; Liang, Z.; Ma, X.; Liang,
724 X.-J., Multifunctional aptamer-based nanoparticles for targeted drug delivery to circumvent
725 cancer resistance. *Biomaterials* **2016**, 91, (C), 44-56.
- 726 107. Li, Q. S.; Zhao, D.; Shao, X. R.; Lin, S. Y.; Xie, X. P.; Liu, M. T.; Ma, W. J.; Shi, S. R.; Lin, Y. F.,
727 Aptamer-Modified Tetrahedral DNA Nanostructure for Tumor-Targeted Drug Delivery.
728 *ACS Appl. Mater. Interfaces* **2017**, 9, (42), 36695-36701.
- 729 108. Jain, R. K.; Stylianopoulos, T., Delivering nanomedicine to solid tumors. *Nat. Rev. Clin. Oncol.*
730 **2010**, 7, (11), 653-664.
- 731 109. Jiang, Q.; Song, C.; Nangreave, J.; Liu, X.; Lin, L.; Qiu, D.; Wang, Z.-G.; Zou, G.; Liang, X.;
732 Yan, H.; Ding, B., DNA origami as a carrier for circumvention of drug resistance. *J. Am. Chem.*
733 *Soc.* **2012**, 134, (32), 13396-13403.
- 734 110. Zhao, Y.-X.; Shaw, A.; Zeng, X.; Benson, E.; Nyström, A. M.; Högberg, B., DNA origami
735 delivery system for cancer therapy with tunable release properties. *ACS Nano* **2012**, 6, (10),
736 8684-8691.
- 737 111. Halley, P. D.; Lucas, C. R.; McWilliams, E. M.; Webber, M. J.; Patton, R. A.; Kural, C.; Lucas,
738 D. M.; Byrd, J. C.; Castro, C. E., Daunorubicin-Loaded DNA Origami Nanostructures
739 Circumvent Drug-Resistance Mechanisms in a Leukemia Model. *Small* **2015**, 12, (3), 308-320.
- 740 112. Wang, P.; Rahman, M. A.; Zhao, Z.; Weiss, K.; Zhang, C.; Chen, Z.; Hurwitz, S. J.; Chen, Z.
741 G.; Shin, D. M.; Ke, Y., Visualization of the Cellular Uptake and Trafficking of DNA Origami
742 Nanostructures in Cancer Cells. *J. Am. Chem. Soc.* **2018**, 140, (7), 2478-2484.
- 743 113. Zhang, Q.; Jiang, Q.; Li, N.; Dai, L.; Liu, Q.; Song, L.; Wang, J.; Li, Y.; Tian, J.; Ding, B.; Du, Y.,
744 DNA origami as an in vivo drug delivery vehicle for cancer therapy. *ACS Nano* **2014**, 8, (7),
745 6633-6643.
- 746 114. Jiang, Q.; Shi, Y.; Zhang, Q.; Li, N.; Zhan, P.; Song, L.; Dai, L.; Tian, J.; Du, Y.; Cheng, Z.; Ding,
747 B., A Self-Assembled DNA Origami-Gold Nanorod Complex for Cancer Theranostics. *Small*
748 **2015**, 11, (38), 5134-5141.
- 749 115. Perrault, S. D.; Shih, W. M., Virus-Inspired Membrane Encapsulation of DNA
750 Nanostructures To Achieve In Vivo Stability. *ACS Nano* **2014**, 8, (5), 5132-5140.
- 751 116. Huang, X.; Jain, P. K.; El-Sayed, I. H.; El-Sayed, M. A., Plasmonic photothermal therapy
752 (PPTT) using gold nanoparticles. *Lasers Med. Sci.* **2007**, 23, (3), 217-228.

753117. Liu, J.; Song, L.; Liu, S.; Jiang, Q.; Liu, Q.; Li, N.; Wang, Z.-G.; Ding, B., A DNA-Based
754Nanocarrier for Efficient Gene Delivery and Combined Cancer Therapy. *Nano Lett.* **2018**, 18,
755(6), 3328-3334.